

Application of regional activity estimation (REGAE) to verbal working memory ERP data using fMRI-selected regions of interest

M.E. Pflieger¹, K.A. Moores², R.E. Greenblatt¹, C.R. Clark²

¹Source Signal Imaging, Inc., San Diego, USA

²The Flinders University of South Australia, Adelaide

Poster presented at the 9th Annual Meeting of the Cognitive Neuroscience Society, San Francisco, April 16, 2002

Correspondence:

Mark E. Pflieger

2323 Broadway, Suite 102

San Diego, CA 92102 USA

email: mep@sourcesignal.com

phone: +1-619-234-9935 ext 15

<http://www.sourcesignal.com/>

Introduction

Because EEG/ERP and fMRI are complementary modalities with respect to space/time resolution, there is considerable interest in combining information from both techniques [1]. Ideally, we seek a hybrid methodology that has the spatial resolution of fMRI and the temporal resolution of EEG. Three major strategies are:

1. Make *joint* inferences about underlying brain activity via unified fMRI/EEG analysis
2. Inform fMRI analysis using temporal results from EEG analysis
3. Inform EEG analysis using spatial results from fMRI analysis

Strategy 1 has the most ambitious objective—true *fusion* of EEG and fMRI. A natural framework is Bayesian statistics [2]. This ultimately depends, however, on a well-developed and balanced theory of how brain activity produces both EEG and fMRI signals.

Strategy 2: A promising approach is to record simultaneous EEG/fMRI and then to incorporate EEG features (e.g., via FFT analysis) into the design matrix when making the fMRI statistic image [3]. However, this discards the millisecond resolution of EEG.

Strategy 3 typically uses fMRI to constrain the global EEG inverse problem. The objective of this study is to illustrate a distinctly different sub-strategy: *Use fMRI to select regions of interest (ROIs) for local EEG source estimation.*

Comparison of constraint versus selection hinges on the distinction between global versus local source estimation. Global source estimation finds a source distribution in the brain that *models all* scalp EEG data (except noise). The source distribution can be overdetermined and discrete (e.g., a relatively small number of equivalent current dipoles), or it can be underdetermined and distributed (e.g., cortically constrained current density). In the overdetermined case, a globally unique solution (best-fitting source model) may exist, but is generally difficult to find (in a “haystack” of local minima). Thus, fMRI can assist in finding the global solution by “seeding” dipoles in hotspots (e.g., [6]). In the underdetermined case, many solutions model the data equally well (after regularizing for noise), so we require a mathematical norm (e.g., minimum norm, maximum smoothness) to select the “best” solution. Here, information from fMRI can weight (or bias) the norm.

Local source estimation aims to estimate activity in pre-selected ROIs: The goal is *not* to find a global source model of the scalp data. In global estimation, all source elements function together to model the data. In local estimation, by contrast, activity in each ROI is estimated *independently* of any other ROI. Consequently, the use of fMRI to *select* ROIs is not at all the same as

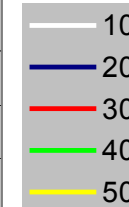
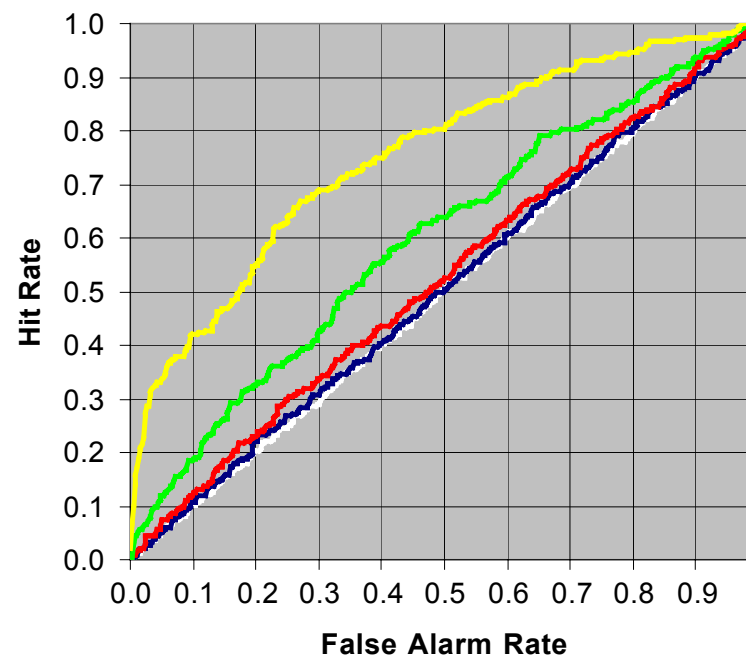
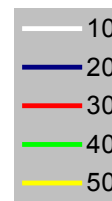
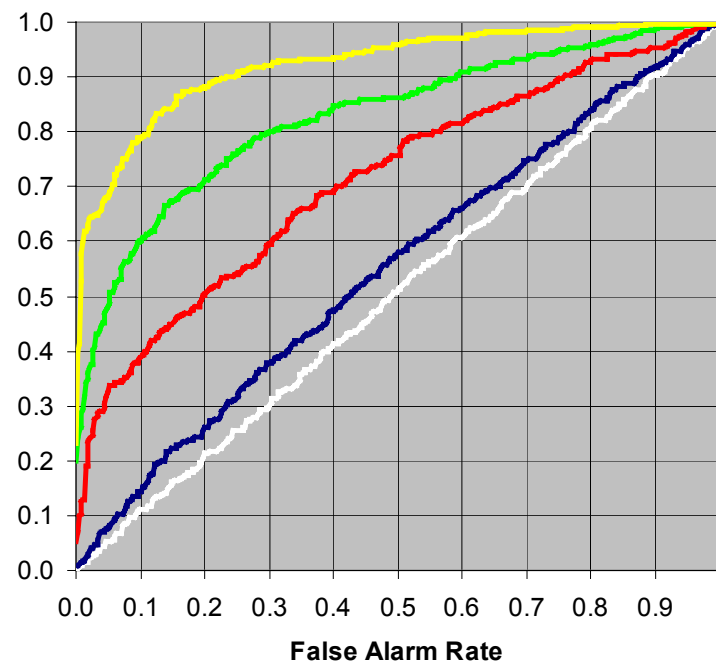
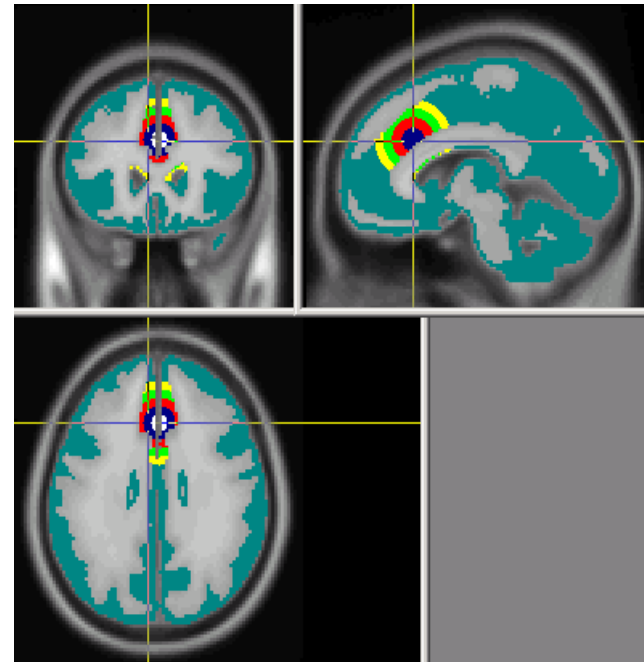
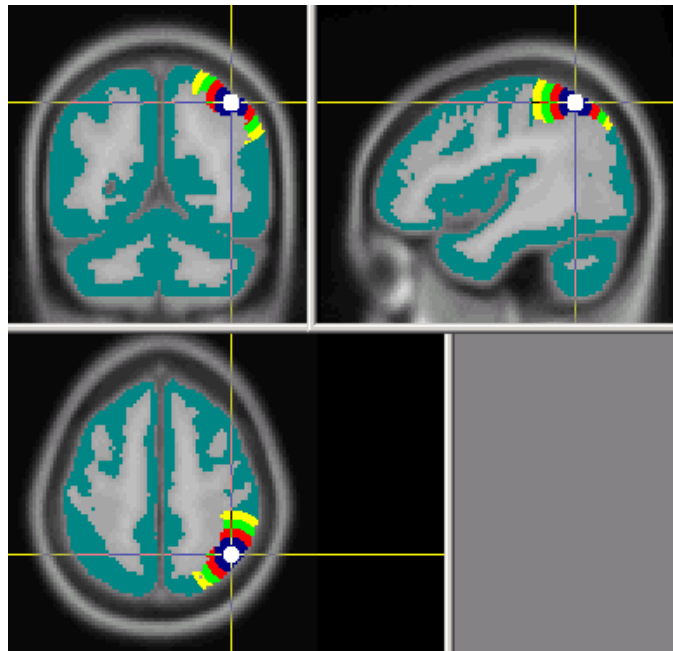
constraining global inverse solutions. The former uses *EEG data only* to estimate ROI activity. Thus, the net result is a set of *spatial activations* that depend only on *fMRI* data, and a corresponding set of *source time series* that depend only on *EEG/ERP* data. In some ways, this approaches the goal of the ideal hybrid spatiotemporal resolution—however, see Discussion below.

Strategy 3: Inform EEG analysis using spatial results from fMRI analysis

- Constrain the *global* EEG inverse problem
 - *Overdetermined model*: Seed dipoles in fMRI hotspots
 - *Underdetermined model*: Use fMRI-weighting to bias a cortical current density solution
- Use fMRI to select ROIs for *local* source estimation

REGAE

Here we apply a new method of local source estimation, *REGional Activity Estimation* (REGAE, [4]) to fMRI-selected ROIs.

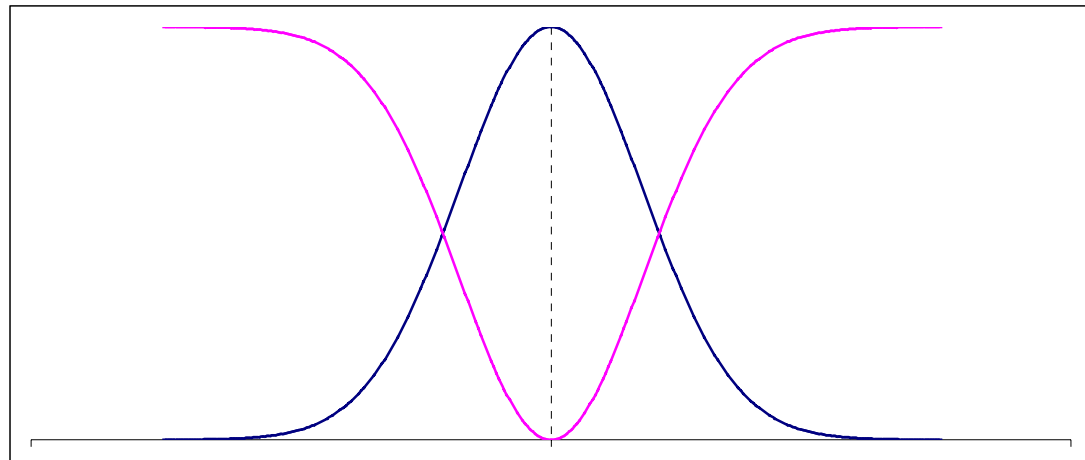


For each ROI, REGAE seeks to balance an inevitable tradeoff between *spatial resolution*, as measured by the spread of a region around a location in gray matter, and *discriminability* between intra-ROI and extra-ROI activity, as measured by the area under a suitably constructed receiver operator characteristic curve (AUROC). An ROI centered on a location has a minimum effective size, below which discriminability performance is no better than chance (AUROC = 0.5), and above which discriminability increases eventually to near perfect performance (AUROC = 1.0). Specific resolution/discriminability characteristics depend principally on the ROI location in the brain, the EEG electrode configuration, and the source space model of gray matter. Thus, in order to match (i.e., equalize) discriminability characteristics, spatial resolution must vary across brain regions.

These ideas are illustrated at left. Parietal and anterior cingulate ROIs are shown with 5 spatial spreads (10 – 50 mm, FWHM), and with corresponding ROC curves. Discriminability (AUROC) increases with loss of spatial resolution (increase of spread). The parietal ROI has better signal detection characteristics due to its location.

Computation of a REGAE estimator

A REGAE estimator for a region of interest (ROI) is a matrix \mathbf{E} of size d (estimation space dimension) by m (number of channels). The estimation space generally has more than one dimension because the region is extended in space, which provides several degrees of freedom for current flow in gray matter. Given an EEG measurement $\mathbf{v}(t)$ at time t , the ROI activity estimate at time t is $\mathbf{E}\mathbf{v}(t)$ —a vector in d -dimensional estimation space. The total activity at time t is $|\mathbf{E}\mathbf{v}(t)|$, a non-negative scalar. To compute \mathbf{E} , first the source space is



divided into ROI and non-ROI regions. A fuzzy region may be defined via a gaussian distribution that surrounds a point of interest (POI) in 3 dimensions. Shown at left is a 1D ROI (blue) and its complementary non-ROI (pink). As illustrated in the previous frame, the ROI is the intersection of a gaussian distribution with the source space (gray matter).

Spatial spread may be measured via σ , the gaussian standard deviation, or via the gaussian full width at half maximum (FWHM). Assuming maximum entropy statistics on the source space (i.e., independent and identically distributed activity throughout), ROI and non-ROI covariance matrices are projected to the EEG measurement space via a volume conductor model of the head, and a ROI versus non-ROI *discrimination matrix* is formed from these two. The estimator matrix \mathbf{E} is obtained via singular value decomposition (SVD) of the discrimination matrix. A free parameter γ , useful for fine-tuning the ROC curve, is the power to which the singular values are raised. Estimation units are not physical units, but typically are normalized.

Task & Data Acquisition

EEG and fMRI data were analyzed from a single subject (age 21.5 years, IQ normal, no history of head injury or psychological/neurological illness), who participated in an experiment designed to identify the locations and activity time courses of brain regions involved in the *updating of verbal working memory* (c.f., reference [5]).

Task: Pseudo-random sequences of words were presented visually in a randomized case (upper or lower) at a fixed intensity (300 ms duration, SOA = 1600 ms \pm 200 ms) in blocks of 32 words, with 4 target words per block. Word sequences were identical in structure and form across all blocks, with only the task instructions and words varying between blocks. The subject was instructed to respond to target words using a right index finger button press. At the beginning of each block, instructions

Fixed Target (FT) condition: Target words were defined at the beginning of a block as a particular word in the attended case (“oddball”). Thus, the FT condition required the subject to hold a single target word in working memory for the duration of a block.

Variable Target (VT) condition: A target was defined as the consecutive repeat of any word in the attended case (“two-in-a-row”). Thus, the VT condition required the subject to update working memory continually.

were to attend to words in a nominated case (upper or lower; this manipulation was designed to minimize the use of iconic memory and to increase the word presentation rate). There were 8 runs (320 s each) of 6 blocks each. Two conditions (FT versus VT, see box at left) were randomized across blocks.

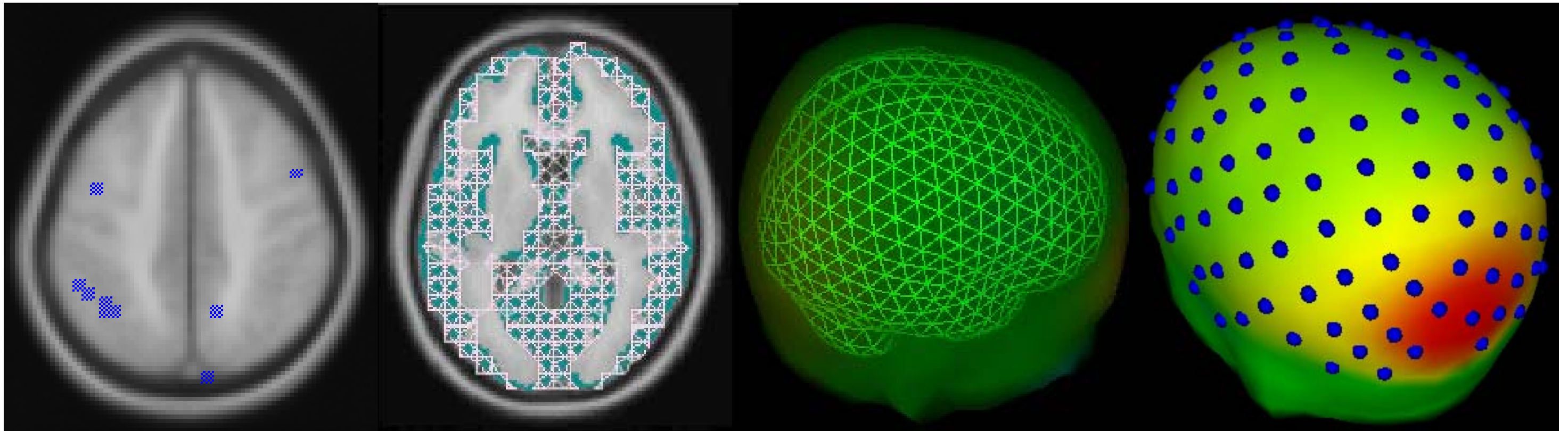
MRI acquisition and processing. High resolution structural MRI was collected using a conventional MPRAGE sequence. Whole brain fMRI data were acquired in 320 s runs (80 acquisitions per run) using a gradient echo EPI sequence (TR = 4 s, TE = 51 ms, flip angle = 90°, FOV = 500 \times 375 mm, 128 \times 96 pixels, voxel size = 3.91 \times 3.91 \times 7 mm, no interslice gap, interleaved slice acquisition). After acquisition, individual fMRI volumes underwent motion detection, motion correction, and global normalization. Hypotheses were tested (within subject) using

the nonparametric Kolmogorov-Smirnov test between VT and FT conditions. The subject’s z-map was thresholded at a RESEL threshold of $p < 0.05$ (one tailed). AIR (AIR 3.0, Woods, 1992) was used to align (6 df) subject statistical maps (which were resampled to 1 \times 1 \times 1 mm) to the high resolution MRI. The individual MRI was then aligned to the MNI Template using a 12 df alignment.

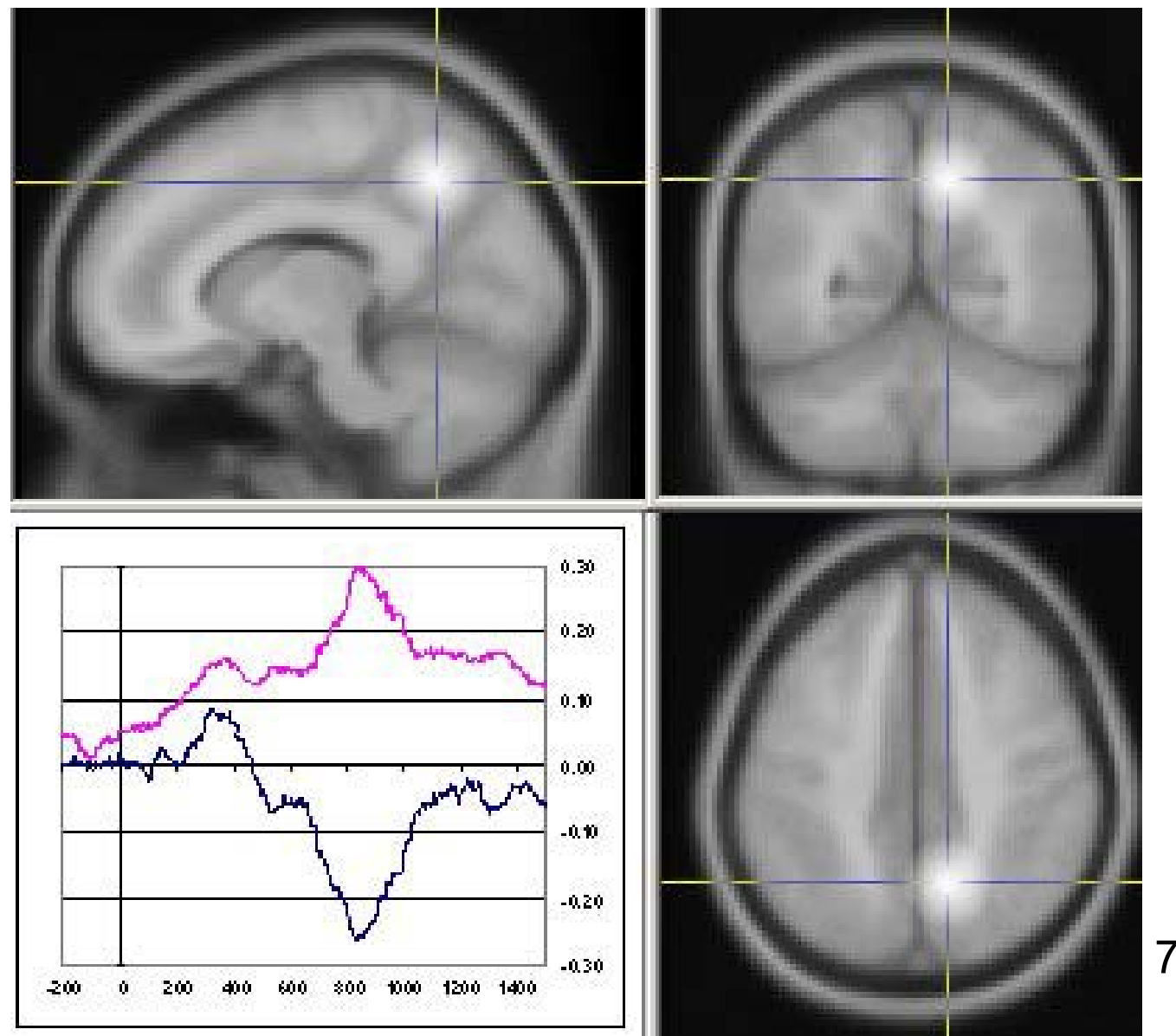
EEG acquisition and early processing. EEG was acquired continuously in a separate session (124 channels, DC-70 Hz bandpass, 500 Hz digitization rate, 1000 gain, 16 bit AD resolution). Single trial EEG was epoched from 200 ms pre-stimulus to 1500 ms post-stimulus. Ocular artifacts were corrected via linear regression. Epochs with excessive EEG activity ($\pm 120 \mu\text{V}$) or reaction times indicative of anticipatory (<100 ms) or slow (>900 ms) responses were rejected. Remaining epochs were baselined on the 200 ms pre-stimulus interval and averaged to estimate event-related potential (ERP) activity at the scalp for each condition (FT and VT). Electrode location coordinates were determined via a magnetic digitizer.

REGAE analysis

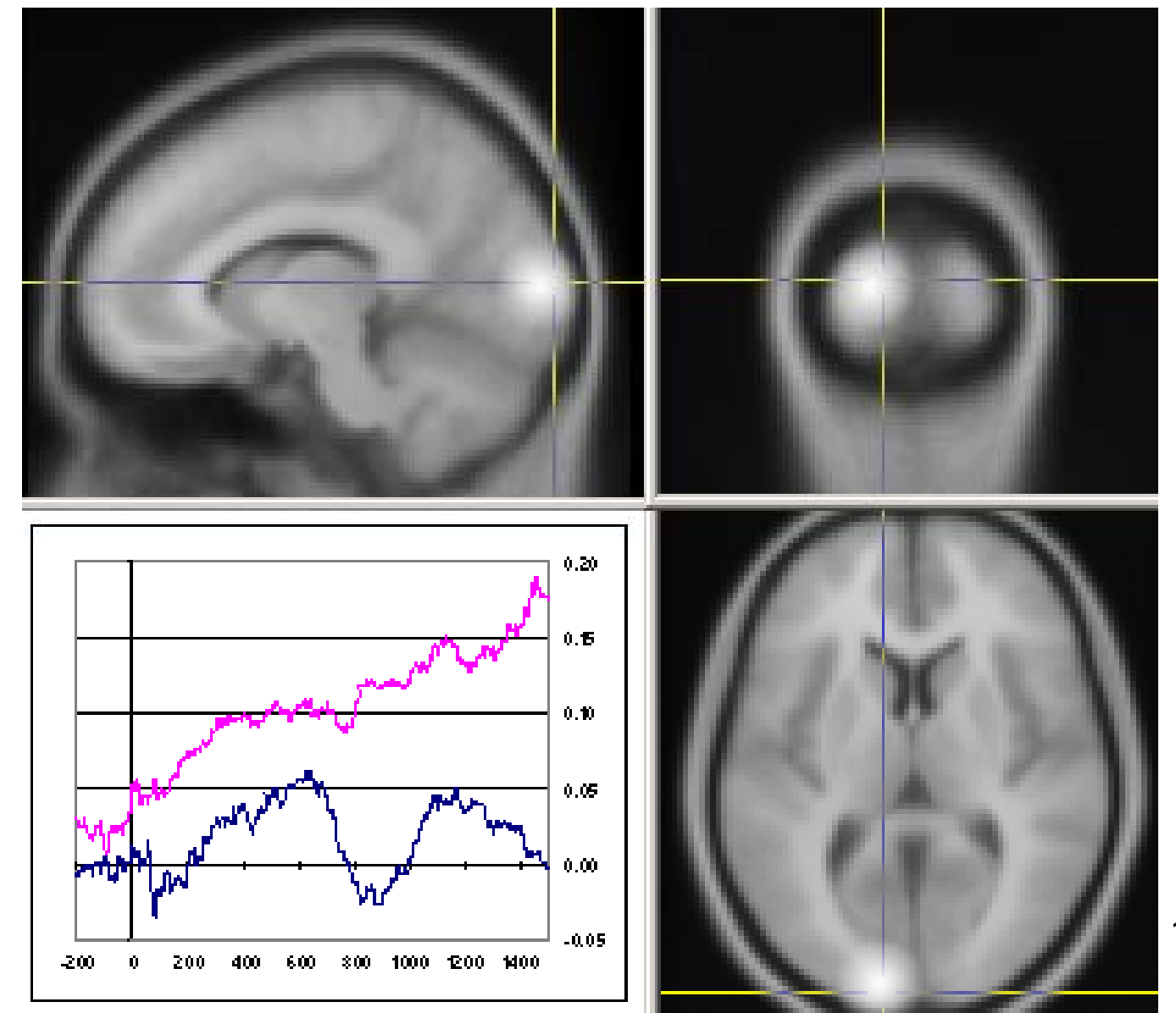
Digitized electrode locations were co-registered with the MNI average head. A source space model was constructed by (a) making a gray matter segmentation of the MNI average brain, (b) generating a tetrahedral mesh within this volume (supervoxels with 7 mm edge length, 4,939 locations), and (c) placing three dipole elements (with x, y, and z orientations) at each mesh location. A boundary element head model was constructed (3 shells: inner skull, outer skull, and scalp), and the complete forward matrix computed (124 channels \times 14,817 dipole elements). *The thresholded fMRI, co-registered with the MNI average brain, was used to select **16 points of interest (POIs)***. (All of the preceding steps employed standard functions of EMSE 5.0.) Using prototype software, REGAE estimators were tuned for each POI by adapting the spatial spread to achieve a uniform ROI discriminability of AUROC = 0.9 ($\gamma = 0.25$, estimator dimension = 12, 100 trials per ROC curve). The resulting spatial spreads (gaussian standard deviations) ranged from $\sigma = 13$ mm (for POI 5, located in superficial lateral parietal cortex) to $\sigma = 32$ mm (for POI 16, located deep within the calcarine fissure). The estimators were applied to the FT, VT, and VT-FT scalp ERP data. In addition, the difference of total estimated activities was formed (that is, Est(VT)-Est(FT)).



The figures below show the VT-FT difference results for six POIs. For each POI, the top trace (pink) is the estimated activity for the scalp difference ERPs, and the bottom trace (blue) is the difference between the estimated activities for each ERP condition. Thus, the bottom trace is the between-condition difference in total estimated ROI activity (positive values indicate more total activity in the VT condition, negative values indicate more total activity in the FT condition), whereas the top trace reflects the norm (nonnegative values) of the difference between 12-dimensional estimator vectors (which takes “spatial phase” into account). The bottom trace rectified cannot exceed the top trace. Images use the radiological convention (right is left).

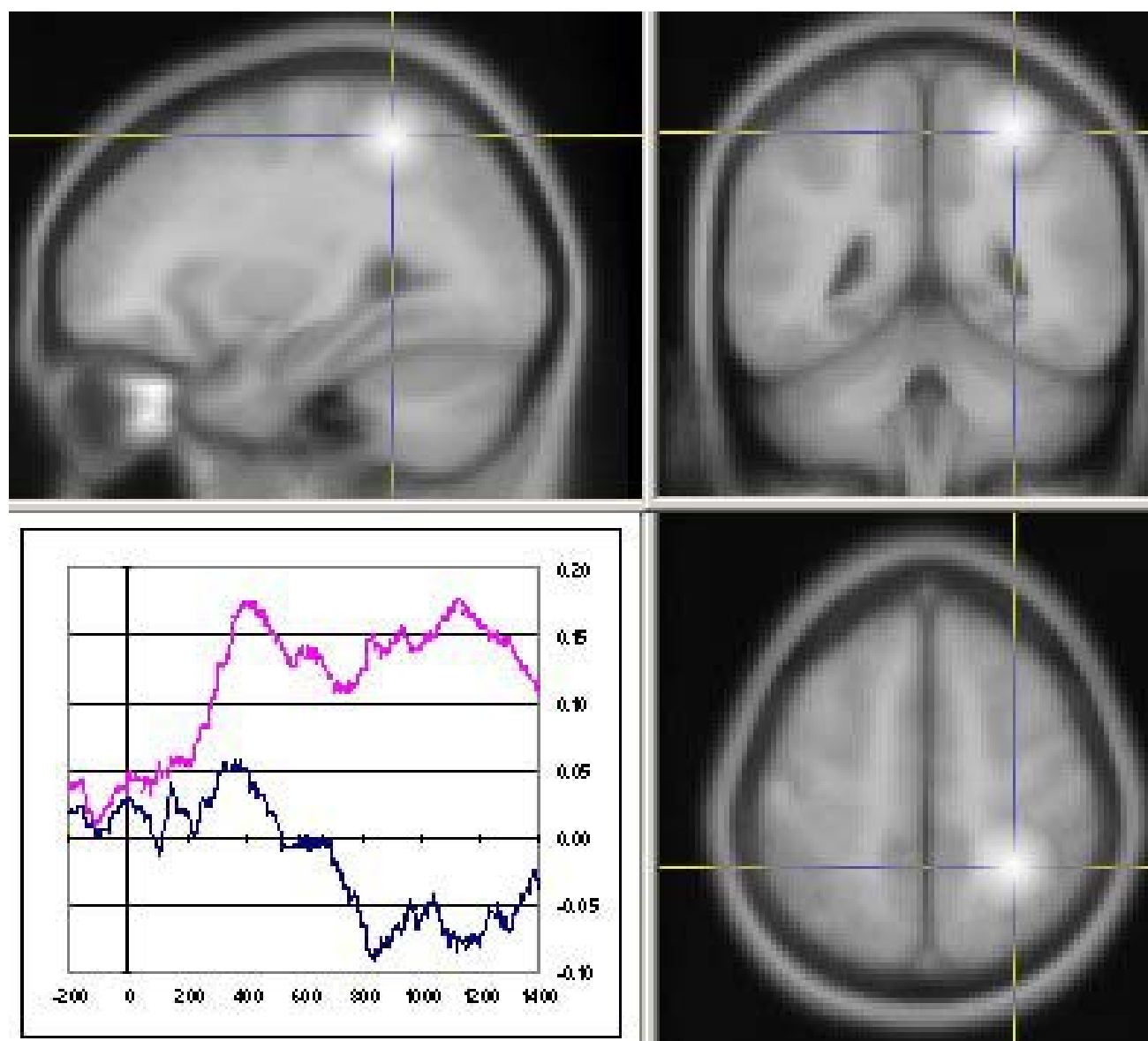


7

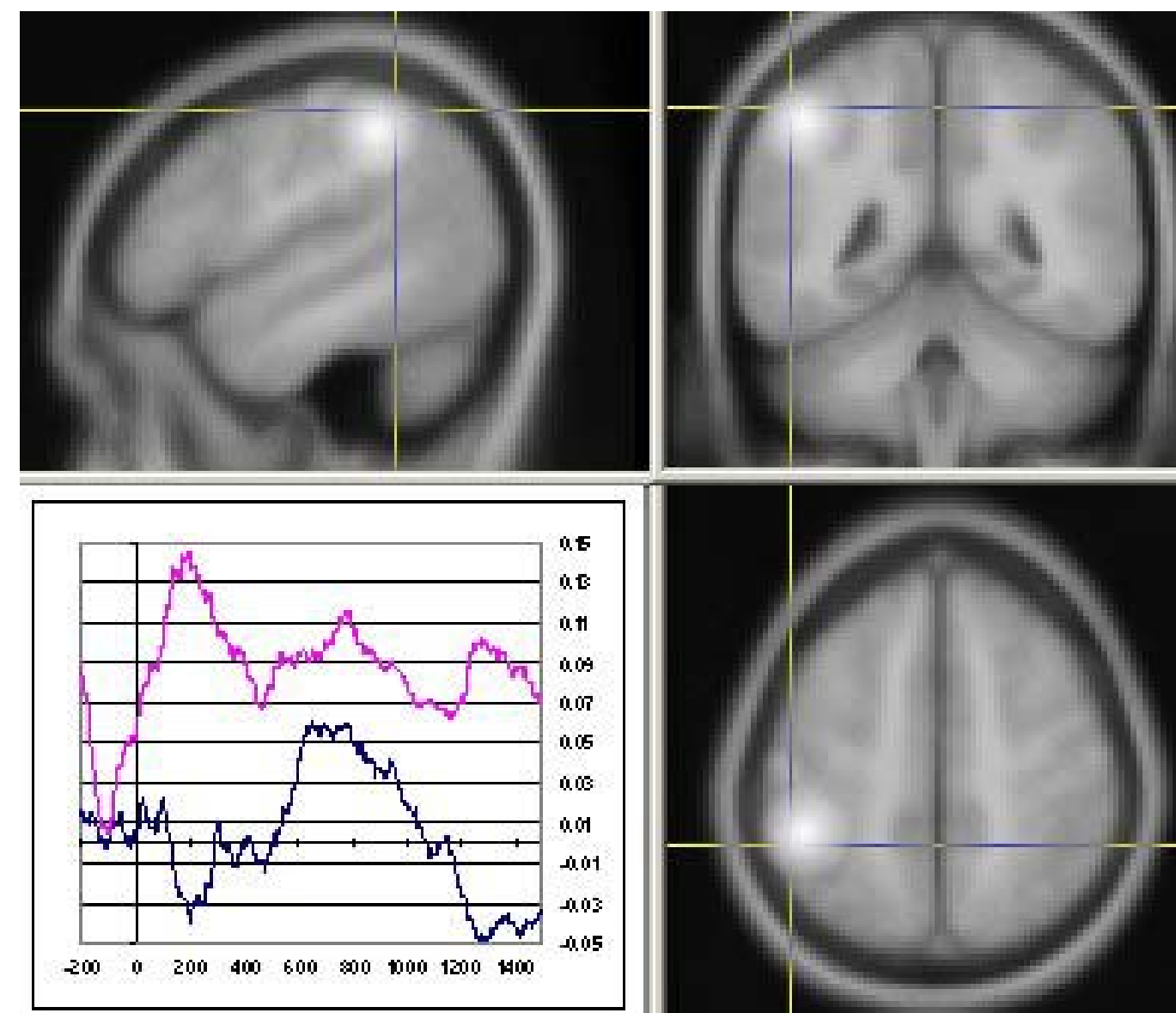


14

POI 7 (left medial parietal, $\sigma = 14.5$ mm) shows the largest differences: VT > FT early (peaking about 390 ms), but VT < FT later (peaking about 870 ms). POI 14 (right visual cortex, $\sigma = 20$ mm) shows VT > FT predominantly, except for early latencies (~80-200 ms) and a dip around 900 ms.

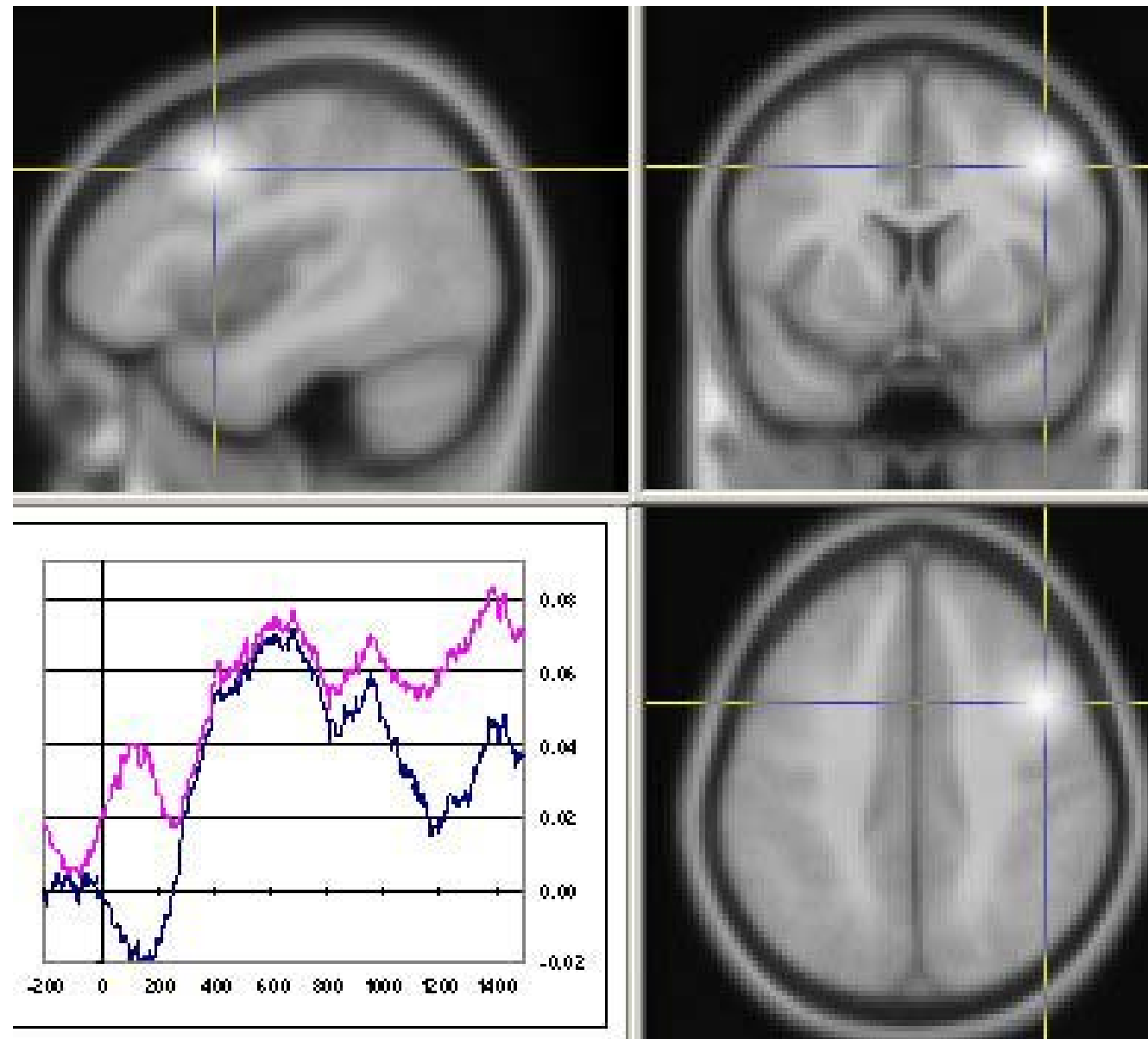


4

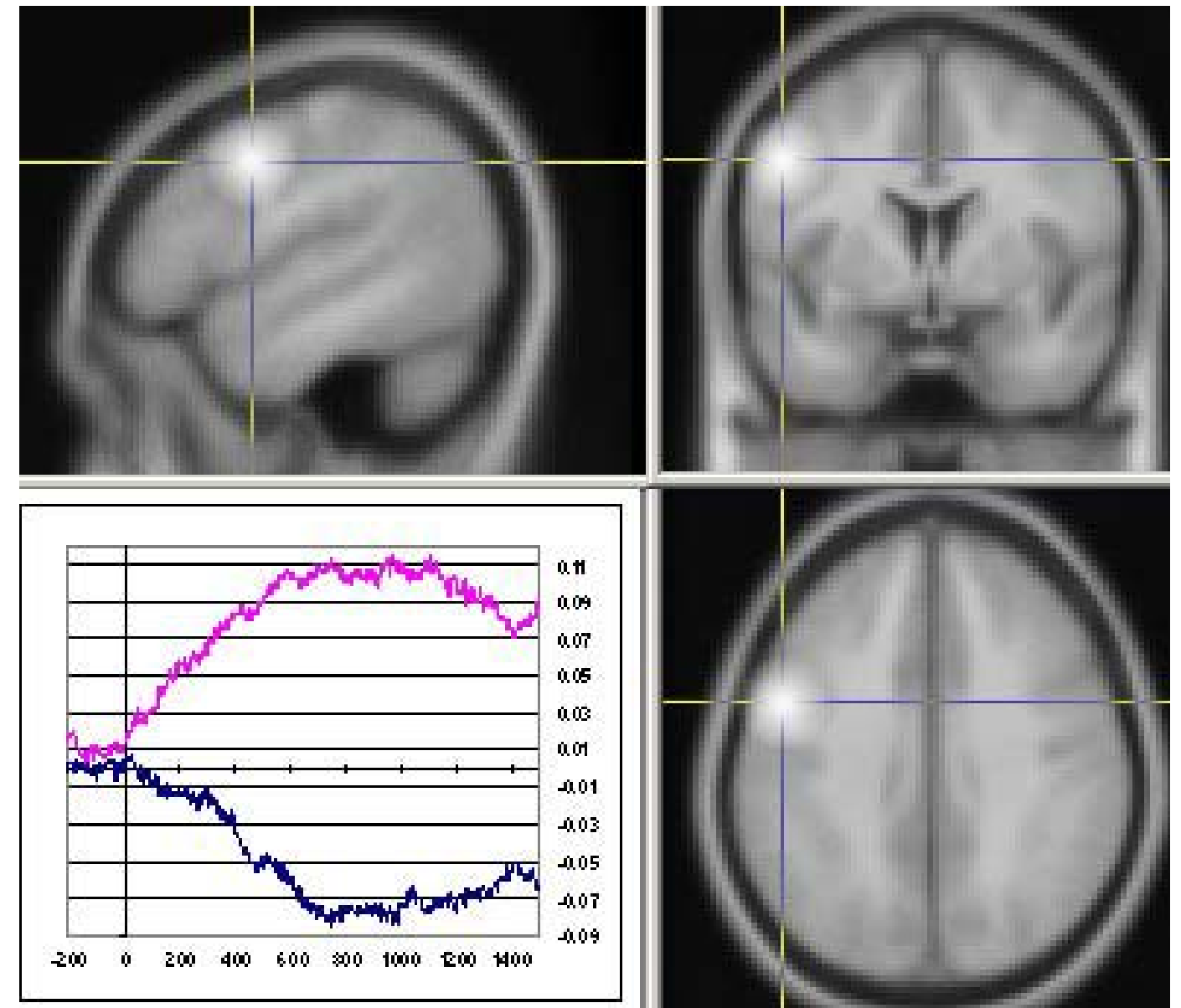


5

POI 4 (left lateral parietal, $\sigma = 17.5$ mm) and POI 5 (right lateral parietal, $\sigma = 13$ mm) have *opposite tendencies*. The left side (shown on the left) shows $VT > FT$ early (< 500 ms) and $VT < FT$ later, whereas the right side is approximately the reverse (with a return, however, to $VT < FT$ at about 1200 ms).



8



9

POI 8 (left lateral frontal, $\sigma = 14.6$ mm) and POI 9 (right lateral frontal, $\sigma = 17.5$ mm) also display different tendencies. On the left side (shown on the left), $VT < FT$ early (< 260 ms), and $VT > FT$ thereafter. On the right, $VT < FT$ throughout the interval. For each of these regions, the near equivalence of the pink trace with the rectified blue trace (rectification not shown) implies that the difference between conditions is almost purely quantitative. That is, the configurations of intra-regional current flow are nearly the same between conditions.

Discussion

Whereas fMRI analysis looks for a predominance of one inequality ($VT > FT$ versus $FT > VT$) integrated over a period of time, our results illustrate the likely possibility that *event-related activity differences in a region may change polarity on a time order of hundreds or perhaps tens of milliseconds*. Thus, when it comes to timing, EEG can treat several subtle possibilities that this fMRI analysis (block design) cannot address. On the other hand, the spatial resolution of the EEG REGAE technique is much coarser than fMRI, and thus the estimated activities include surrounding brain areas that were excluded the fMRI analysis.

These temporal and spatial differences may account for some anomalies. For example, the REGAE estimates for POI 9 show VT consistently less than FT; however, the fMRI activations were selected using a one-tailed test for $VT > FT$. Two possibilities are: (a) the polarity could change outside the time interval (~ 1 s) used for the ERP analysis, or (b) $VT > FT$ might be focal to the fMRI activated area, with $FT > VT$ in the surrounding area.

There are additional possibilities. Implicitly, we have supposed that all neuroelectric activities are equivalent with respect to hemodynamics. However, we can ask: *Do different frequencies of neuroelectric activity contribute equally to hemodynamic responsiveness?* For example, slow shifts from the prestimulus baseline in this DC recording play a large role in the REGAE estimated activities, especially at longer latencies. Is the metabolic cost

equivalent for low versus high frequency neuroelectric activity? Alternatively, should we have convolved the EEG data with the estimated fMRI hemodynamic response function (a low pass filter) in order to expect comparable results? These questions can be addressed in a future study by filtering the EEG prior to REGAE analysis, and asking: Which temporal filter applied to the EEG data produces REGAE estimates of activity that are most consistent with the sign of the fMRI activations?

A further subtlety is the distinction between *quantitative differences in total activity* (blue traces) versus *differences that incorporate current flow configurations* (pink traces). The results imply that some REGAE VT – FT differences are not merely quantitative, but involve flow configuration changes. Presumably, however, fMRI is sensitive to total activity only.

In a recent paper, dipoles were seeded in fMRI activations to model scalp data and to estimate source time series [6]. By contrast with REGAE, the solution for each source time series depends on the adequacy of the full model. For multiple dipole models in general, spatial interaction of errors increases with the number of active sources [7].

To conclude from a methodological perspective: Use of REGAE to estimate activity in fMRI ROIs provides a fresh point of view, which raises further questions about how EEG and fMRI “see” underlying brain activity. See [5] for a discussion of related cognitive issues.

References

- [1] See *IJBEM* 3(1), entire issue, <http://ee.tut.fi/rgi/ijbem/volume3/number1/>
- [2] Trujillo-Baretto NJ, Martínez-Montes E, Melie-García L, Valdés-Sosa PA (2001): A symmetrical Bayesian model for fMRI and EEG/MEG neuroimage fusion. *IJBEM* 3(1).
- [3] Goldman R, Stern J, Engel J Jr, Cohen M (2001): Tomographic mapping of alpha rhythm using simultaneous EEG/fMRI. *NeuroImage* 13(6): S1291 (abstract).
- [4] Pflieger ME, Greenblatt RE (2001): A regional approach to M/EEG source estimation: Characterizing the tradeoff between spatial resolution and signal discriminability. *NeuroImage* 13(6): S219 (abstract).
- [5] Clark CR, Moores KA, Lewis A, Weber DL, Fitzgibbon S, Greenblatt R, Brown R, Taylor J (2001): Cortical network dynamics during verbal working memory function. *Int J Psychophysiol* 42: 161-76.
- [6] Opitz B, Rinne T, Mecklinger A, von Cramon DY, Schröger E (2002): Differential contribution of frontal and temporal cortices to auditory change detection: fMRI and ERP results. *NeuroImage* 15:167-74.
- [7] Mosher JC, Spencer ME, Leahy RM, Lewis PS (1993): Error bounds for EEG and MEG dipole source localization. *Electroencephalogr Clin Neurophysiol* 86: 303-21.

Acknowledgement

This work is supported by a grant from the NIMH (1-R43-MH-64343-1).